Innovative FT-IR Imaging of Protein Film Secondary Structure before and after Heat Treatment

EMILY S. BONWELL AND DAVID L. WETZEL*

Microbeam Molecular Spectroscopy Laboratory and Grain Science Department, Kansas State University,
Manhattan, Kansas 66506

Changes in the secondary structure of globular protein occur during thermal processing. An infrared reflecting mirrored optical substrate that is unaffected by heat allows recording infrared spectra of protein films in a reflection absorption mode on the stage of an FT-IR microspectrometer. Hydrated films of myoglobin protein cast from solution on the mirrored substrate are interrogated before and after thermal denaturation to allow a direct comparison. Focal plane array imaging of 280 protein films allowed selection of the same area in the image from which to extract spectra. After treatment, 110 of 140 spectra from multiple films showed a dramatic shift from the α-helix form (1650 $\pm$ 5 cm^{-1}) to aggregated forms on either side of the original band. Seventy maxima were near 1625 cm^{-1}, and 40 shifted in the direction of 1670 cm^{-1}. The method developed was applied to films cast from two other commercial animal and plant protein sources.

KEYWORDS: FT-IR microspectroscopy; protein secondary structure; infrared protein film analysis; thermal processing of protein; infrared imaging

INTRODUCTION

It is well-known from vibrational spectroscopic data that upon heating protein occurring in the α-helix form of secondary structure in nature aggregates, producing an increase in the intermolecular antiparallel β-sheet form accompanied by a decline in the α-helix form (*1−5*). Protein thermal processing treatments such as extrusion, pasteurization, baking, and canning involve denaturation. Analysis of this process is manifested spectroscopically by the appearance of amide I infrared bands in the 1680−1670 cm^{-1} region and/or the 1620 cm^{-1} region (*6, 7*). Synchrotron FT-IR microspectroscopy has been applied in situ to differentiate β-amyloid plaque in Alzheimer's diseased brain tissue from surrounding healthy tissue (*8*). It has also been applied to wheat subaleurone endosperm to determine the ratio of α-helix to β-sheet in reference to hard wheat protein quality for end use among breeding lines (*8−11*).

A previously reported series of spectra of myoglobin taken after treatment at various temperatures from 20 to 90 °C (*12*) showed only the α-helix band at ca. 1658 cm^{-1} at temperatures from 20 to 68 °C. At 70 °C, emergence of a band at 1620 cm^{-1} began, and at temperatures above 73 °C, the 1620 cm^{-1} band predominated as the α-helix band was drastically reduced. Absorption was also observed after heat treatment in the 1680−1670 cm^{-1} region.

Internal reflection with a horizontal internal reflection (ATR) accessory has been the optical technique of choice for infrared analysis before and after thermal processing (*13−18*). This entails positioning the film in optical contact with the internal reflecting crystalline surface of the ATR substrate before and after each stage of thermal treatment. In contrast, the innovative optical procedure described herein enables interrogation of the same location within a protein film before and after treatment. The film is cast on a highly polished stainless steel plate, and mercury cadmium telluride (MCT) focal plane array detection results in a chemical image that enables comparison of spectra before and after treatment for the same proximity near the center of the film. Thus, this study introduces an innovative approach to microspectroscopically reveal and document protein structural changes induced by thermal treatment. With films cast onto a highly polished stainless steel surface, reflection absorption microspectroscopy enables analysis of the same location within the film before and after heating. On the basis of earlier conventional macrospectroscopic studies done in solution (*12*), myoglobin was chosen as a model for our method development because of its relative secondary structural homogeneity and natively high α-helix content. The molecular model developed was subsequently applied to gelatin, another animal protein source, and wheat gluten was used to represent a plant protein source. This study was restricted to the soluble portion of each sample to avoid dealing with more complex insoluble organic materials.

MATERIALS AND METHODS

To follow the conversion of α-helix to other secondary structures during thermal processing, myoglobin films were chosen as a material high in α-helix secondary structure and relatively homogeneous for method development as a model suitable for the study of protein secondary structural changes. Myoglobin had been identified previously as existing primarily as α-helical protein. Films were cast on infrared reflecting glass slides or rigid Teflon followed by drying and removal for transmission microspectroscopy. Unfortunately, those films thick enough to be removed without their destruction were not thin enough to analyze in

---

*Author to whom correspondence should be addressed [telephone (785) 532-6731; fax (785) 532-7010; e-mail dwetzel@ksu.edu].

transmission. The peeled films were rejected, and instead films thin enough for reflection absorption were cast and dried on polished stainless steel (K&S Engineering, Chicago, IL). Preliminary experiments involved films of protein from various sources.

Instrumentation and Materials. All films were imaged using the Perkin-Elmer (Shelton, CT) Spectrum Spotlight IR microscope optically interfaced to a SpectrumOne spectrometer at the Kansas State University Microbeam Molecular Spectroscopy Laboratory. Spectrum software supplied with the imaging system and OMNIC (Thermo-Fisher, Madison, WI) software were used to process the data.

Horse skeletal muscle myoglobin labeled as being of 95−100% purity was obtained from Sigma Aldrich (St. Louis, MO). As described previously (*19*), myoglobin was dissolved, 5% w/w, in 0.01 M phosphate buffer (pH 6.8). Dissolved myoglobin was filtered with a 0.5 μm filter (Millipore, Billerica, MA) using a Sweeney adaptor connected to a 2 mL ground glass syringe. Using a 0.3 mL syringe with a 31 gauge needle, two drops of myoglobin solution were deposited onto polished stainless steel plates, and the liquid was allowed to evaporate at room temperature. This procedure produced a 500−1500 μm diameter film with suitable thickness to allow reflection absorption. Samples were stored in a humidor consisting of a closed vessel containing freshly moistened tissue paper from 30 min to overnight before infrared analysis.

Two other protein materials, gelatin and wheat gluten, were chosen for application of the technique developed. Gelatin in capsule form (0.07 g) (Eli Lilly and Co., Indianapolis, IN) was stirred continuously in 10 mL of deionized water at pH 7.0 until completely dissolved. The gelatin solution was filtered through Whatman no. 1 filter paper, and four drops of filtered gelatin were deposited onto the stainless steel plates to prepare films for imaging.

Wheat gluten of approximately 80% protein content was obtained from MGP Ingredients, Inc. (Atchison, KS). For three films, 1.0 g of gluten was mixed with 10 mL of deionized water at pH 7.0. The mixture was shaken for 2 min and centrifuged at 2500 rpm for 10 min, and the supernatant was recovered. Alternatively, fine grinding of the gluten before mixing with water and longer contact with water were used to increase dissolution.

Procedure. After a background spectrum was collected from the polished plate, reflection absorption measurements of the entire film over 4000−800 cm^{-1} were imaged with 240 and 64 scans co-added, respectively, with a 25 μm image plane masking. The film cast ranged from 500 to 1500 μm in diameter, resulting in up to 4000 spectra. Twenty spectra near the center of each of seven films were evaluated before and after heating for each different protein source for repeatability purposes and to produce a good database.

Thermal processing was done in the presence of water vapor to maintain hydration while allowing changes in protein secondary structure to proceed during heating. After completion of initial imaging, films, mounted on their respective stainless steel plates, were placed in a glass Petri dish (9 cm diameter) containing an inverted watch glass (6 cm diameter) to keep the plate above the water level. Approximately 10 mL of water was poured into the bottom of the dish. A large watch glass (15 cm diameter) covered the Petri dish containing the plate, and the entire apparatus was heated for 30 min at 100 °C. After heating, the plate supporting the film was removed to allow cooling and drying at room temperature for a minimum of 30 min before the same film was imaged using the microspectroscopic parameters previously described. **Figure 1** shows the visible photomicrographs of a myoglobin film before and after heating. In all experiments, the entire film was chemically imaged to select and document the pixels from which spectra were extracted.

Pixel Selection. False color images of the baseline-corrected peak area ratio of protein, from the 1736 to 1500 cm^{-1} region, were produced using Spotlight software (Perkin-Elmer, Waltham, MA) to highlight the spectrally relatively homogeneous central area of the film. Areas high in protein absorbance, typically along the outer "bathtub" ring of the films, were assigned a false red color. This was apparently indicative of three-dimensional self-assembly or aggregation. Twenty spectra from the centermost area of each of seven films were selected for study. Pixels were rejected if their spectrum baseline was slanted or showed serious interference fringes due to the presence of a gap between the film and the stainless steel mirror surface. The center of a few of the films bubbled up after heating, which was apparent from their spectra and from visual
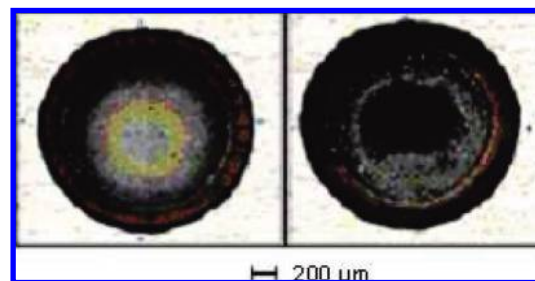

Figure 1. Bright field photomicrographs of the same myoglobin film before (left) and after heat treatment (right).
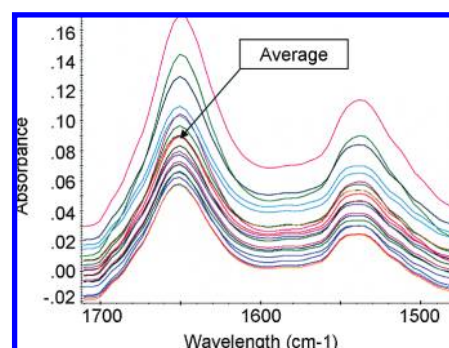

Figure 2. Amide I, II region of 20 spectra (common scale) and the average from a single myoglobin film showing homogeneity before heating.

inspection. In these cases, spectra were extracted from the perimeter of the bubbled area that was still within the center of the film. Twenty spectra per film were averaged, and the peak maxima locations of all 20 spectra and their averages were recorded using Omnic 7.3 software (Nicolet/Thermo Scientific, Madison, WI).

Data Treatment. Second-derivative, deconvolution, and peak fitting were performed on each averaged spectrum using GRAMS AI, 7.02 (Thermo Galactic, Thermo Scientific, Waltham, MA). We detailed this process in previous wheat protein studies (*9*, *10*). The spectral range was reduced to 1782−1570 cm^{-1}. The second derivative using the second order and seven smoothing points identified the position of individual peaks. Each spectrum was deconvolved between 1782 and 1570 cm^{-1} using a gamma factor of 7.5, a value based on results from previous studies (*20*). A mixed Gaussian and Lorentzian function was used to model peaks within the deconvolved spectra using low sensitivity, an offset baseline function, and a full width at half-height (fwhh) of 13 (*20*, *21*). Peaks were fit using 50 iterations. Areas under the model corresponding to α-helix (1650−1660 cm^{-1}) were ratioed to areas of the β-sheet model (1630−1640 cm^{-1}), β-turn/intermolecular antiparallel β-sheet (1670−1685 cm^{-1}), and all peaks other than α-helix summed together.

RESULTS AND DISCUSSION

Myoglobin Model. It is evident from the myoglobin film image results that it is possible to study the effects of thermal processing on the same film deposited on an uncharged reflective substrate. It is widely known that myoglobin exists primarily in an α-helical secondary conformation (*5*, *12*, *22*, *23*). In fact, X-ray crystallographic data confirm that myoglobin consists of >80% α-helix (*24*). For this reason, the relatively homogeneous myoglobin was chosen as a model system to study the effects of thermal processing on protein secondary structure. Twenty spectra from one myoglobin film, in common scale, are overlaid in **Figure 2** to show the homogeneity of myoglobin before heating. **Figure 3** shows false color images of a replicate myoglobin film before and after heating. The ring around the outside perimeter of the film is an area characterized by thicker film deposition where a shift of the amide I band is observed. Spectra extracted from pixels in the
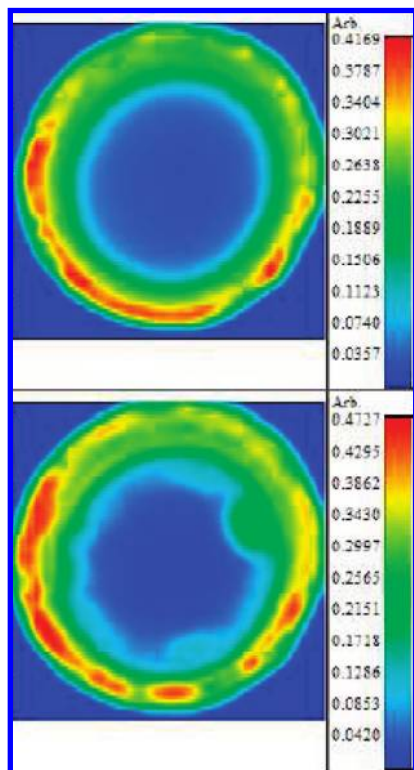
Figure 3. Baseline-corrected 1650 cm^{-1} (amide I) peak area false color images of a single myoglobin film before heating (top) and after heating (bottom). Warm colors on electronic version indicate high-protein areas.
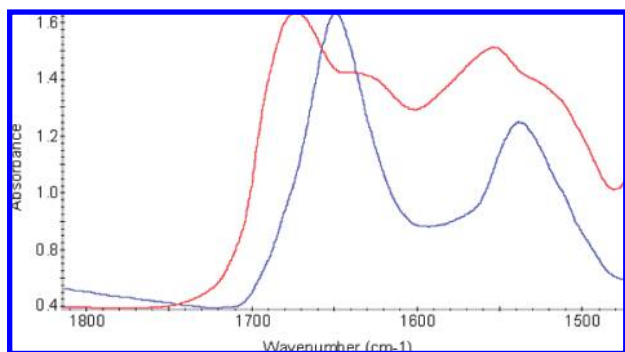

Figure 4. Typical spectrum of the amide I, II region representing the center of an unheated myoglobin film (blue). The spectrum with a 1685 cm^{-1} amide I maximum is typical of the self-assembled protein at the outer edge of the film (red). Spectra from the outer edge were not included in this study.
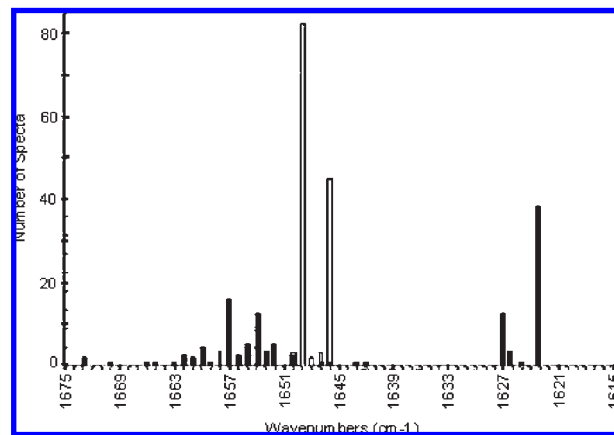

Figure 5. (Open bars) Summation of the amide I peak maxima values for all 140 spectra from seven unheated myoglobins such as those in **Figure 6**. (Solid bars) Summation of the amide I peak maxima of 140 spectra taken from seven myoglobin films heated to 100 °C for 30 min.
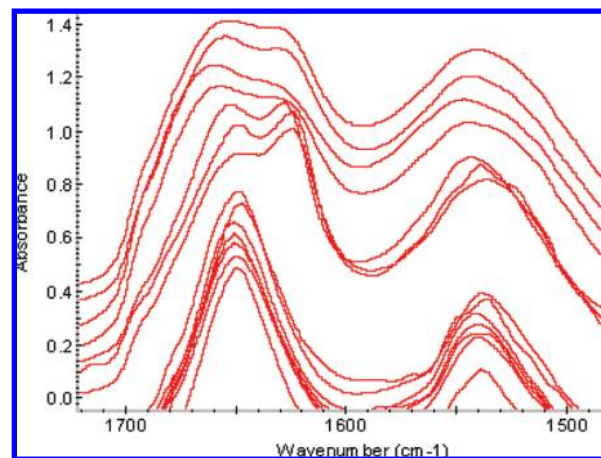

Figure 6. Amide region average spectra from 20 individual spectra extracted from pixels of 7 different unheated myoglobin films (bottom group) and average spectra after heating of the same 7 films (top group).

center of the film, appearing in the electronic version as the dark blue region, have an essentially uniform amide I peak location. A typical spectrum from the outer ring and a typical spectrum from the center region are superimposed in **Figure 4**. As the film dries, there is an apparent continual breaking and re-forming of hydrogen bonds between neighboring protein molecules, air, and surrounding water. Because the outside ring is the first to dry, the protein apparently self-assembles, possibly as intermolecular antiparallel β-sheet or β-turn consistent with the higher frequency band. For simplification, this study was restricted to spectra from the homogeneous center of the film.

Twenty spectra from each of seven different films of myoglobin before heating were compiled into a open band histogram (**Figure 5**) showing most of the spectra with a peak maximum at 1652 and 1648 cm^{-1}. The peak location is consistent with

observations from previous studies (*5*, *12*, *22*, *23*). Upon heating, the amide I band peak maxima (solid bars) shifted to either a higher or lower wavenumber with a distinct shoulder visible. **Figure 6** shows the peak maxima averages from 20–21 spectra of 7 unheated films and 7 heated films. Histograms of the amide I shoulders (**Figure 6**) after heating show a wide distribution compared with the relative uniform spectra obtained before heating. The majority of the spectra in **Figure 6** have shifted to lower wavenumbers, ca. 1625–1630 cm^{-1}, but a substantial portion have also shifted to wavenumbers above 1655 cm^{-1}. During the heating process, proteins unfold. Upon cooling, the hydrogen bonds quickly reunite to maintain the most stable conformation in the shortest amount of time. For this to occur, β-sheet aggregates are favored over α-helical secondary structures. Previous studies of myoglobin in solution (*12*, *23*) have shown that upon heating, the peak location shifts to approximately 1620 cm^{-1} with additional bands appearing at 1685 cm^{-1}, which implies the formation of intermolecular β-sheet aggregates. The present study is in agreement with these findings. In addition, formation of the intermolecular antiparallel β-sheet at around 1670–1680 cm^{-1} has been reported in other proteins (*2*, *4*, *5*).

Interestingly, although the shoulder location predominantly shifted to lower wavenumbers, approximately 12% of the shoulders did not (**Figure 7**). This implies there is not a uniform
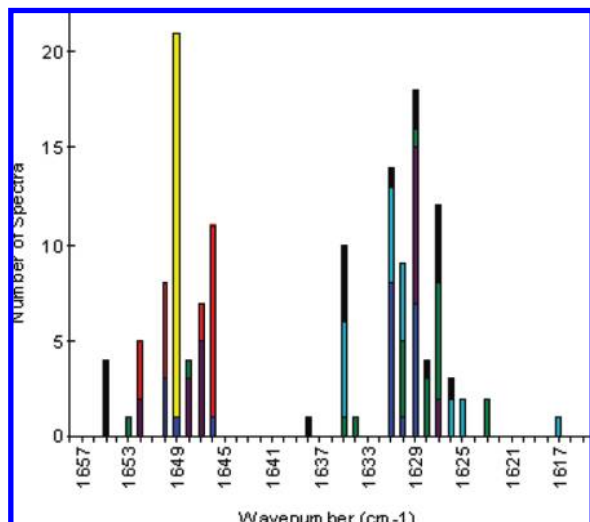
10070 *J. Agric. Food Chem.,* Vol. 57, No. 21, 2009

Bonwell and Wetzel

Figure 7. Location of shoulder on shifted amide I band of spectra from heated myoglobin films (140 spectra in 7 films). In the electronic version, different colors represent contributions from different films.
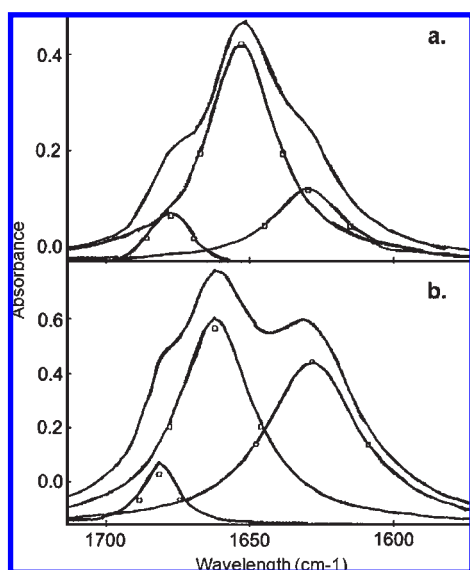

Figure 8. Spectra of protein secondary structure components contributing to the amide I band are modeled from average spectra of myoglobin films before heating (**a**) and after heating (**b**). The models below each actual spectrum in (**a**) and (**b**) were fit into the deconvolved spectra representing different secondary structures. The single component model located at approximately 1655 cm^{-1} representing α-helix is the most prominent in the unheated spectrum (**a**), but diminishes compared to other secondary structure bands that appear after heating (**b**).

conversion from one secondary form to another. When the main peak shifted to a higher wavenumber, a slight amount either stayed in the same spot or shifted to a lower wavenumber, indicating a possible split between α-helix and β-turn and/or intermolecular antiparallel β-sheet aggregates.

Deconvolution results were consistent among all myoglobin films (**Figure 7**). Deconvolution and curve fitting of the average spectra taken from a single film are shown in **Figure 8** before and after heating. It is obvious that the nonheated spectrum is dominated by the α-helix secondary structure at approximately 1653 cm^{-1} and that the β-sheet structure (1630 cm^{-1}) and random coil/turns (1677 cm^{-1}) are less prominent. After heating, how-ever, the α-helix does not completely diminish, but the area ratio
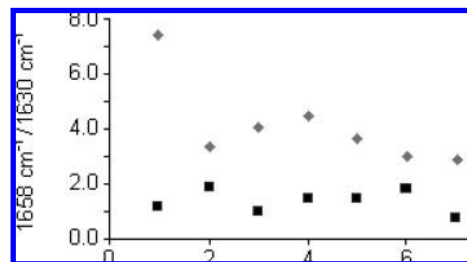

Figure 9. Amide I region of each of seven myoglobin film averages was deconvolved and modeled. Ratios of the areas of α-helix and β-sheet curves fit within this model are plotted to show the difference in ratio between heated (squares) and unheated (diamonds) spectra. In all films, heating diminished the α to β ratio, as well as the ratio of α-helix to all other forms.
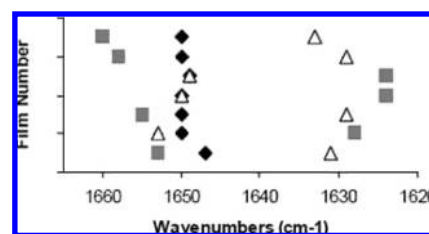

Figure 10. Frequency of the amide I peak maxima of the average spectra taken from seven myoglobin films before (black diamonds) and after (gray squares) heating plotted with the location of the shoulder (open triangles) found in spectra after heating. Before heating, peak maxima indicated by the diamonds are in a relatively straight line at 1650 cm^{-1}.

of α-helix to β-sheet decreases from approximately 3.00 to 1.75, indicative of significant β-sheet formation. At higher frequencies after heating, the random coil/turn peak at 1677 cm^{-1} was replaced with the 1686 cm^{-1} band, which became more promi-nent than the residual α-helix at 1653 cm^{-1}. The shift to the higher wavenumber (1686 cm^{-1}) suggests that intermolecular antipar-allel β-sheet structure formation takes place upon heating. The average results plotted in **Figure 9** show that results are consistent with every myoglobin film. Heating decreases the ratio of α-helix to β-sheet secondary structure in parallel to the ratios of all other protein secondary structures.

Locations of 140 amide I peaks have been plotted for unheated protein films, heated protein films, and shoulders of heated protein films to summarize the extent of secondary structural change of the model protein studied (**Figure 10**). Homogeneity of the film before heating is evident from only a very slight deviation in the peak maxima. After heating, the new peak maxima consistently shifted away from the depleted original peak to a higher or lower wavenumber in approximately equal numbers. Shoulders stay in their original location or shift only slightly. Deconvolution of the amide I region from averaged spectra show that the area of α-helix decreases at the expense of β-sheet and other protein secondary structures upon heating.

Advantages of the Proposed Method and Its Application to Films of Other Proteins. The protein film method developed was subsequently applied to commercial gelatin as another source of mammalian protein and commercial wheat gluten representing a plant source (**Figure 11**). Eight gelatin films were cast that had a predominant population in the 1635 cm^{-1} region prior to thermal processing. The curve-fitted model of **Figure 12** is from a single gelatin film typical of the change in secondary structure contribu-tion. **Figure 13** shows the relative contribution to the amide I band. For each film, the spectra from 25 contiguous pixels were averaged. After heat treatment, six of seven of the protein film
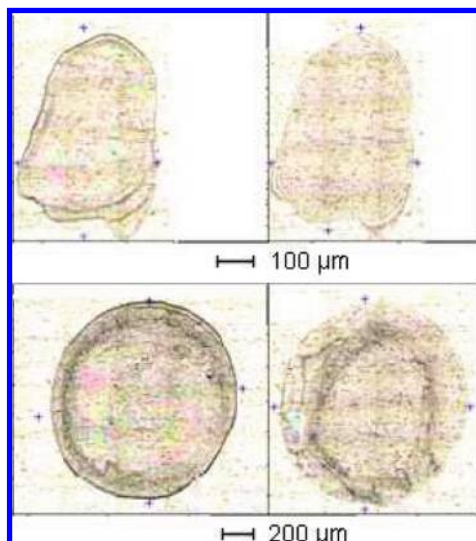
Article

J. Agric. Food Chem., Vol. 57, No. 21, 2009 **10071**

Figure 11. Microscopic images produced using the focal plane array microspectrometer. Films of gelatin (top) and wheat gluten (bottom) are shown before (left) and after (right) heating.
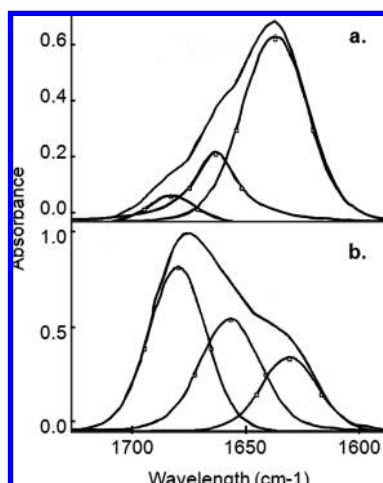

Figure 12. Spectra of protein secondary structure components contributing to the amide I band are modeled from average spectra of gelatin films before heating (**a**) and after heating (**b**). The amide I deconvolved spectra show contributions from protein secondary structure. The models appearing under the actual spectrum were fit into the deconvolved spectra representing different secondary structures. Notice how the model located at approximately 1635 cm^{-1} representing β-sheet secondary structure is the most prominent in the unheated spectrum (**a**), but diminishes compared to that of intermolecular antiparallel β-sheet at approximately 1680 cm^{-1} (**b**).

Figure 13. Frequency of the amide I peak maxima taken from gelatin film spectral averages before (black diamonds) and after (gray squares) heating. Gelatin is homogeneous before heating.

within the center of the film is relatively consistent. After heating, in most cases, amide I absorption is distributed between 1620 and 1685 cm^{-1}, documented as intermolecular antiparallel β-sheets, a common sign of aggregation. The method developed provides options to study the effects of varying temperatures and times of heating of protein films, which may prove useful for future work on food-processing techniques including extrusion, pasteurization, and spray-drying.

An advantage of this microspectroscopic imaging method is the ability to reveal homogeneity or heterogeneity with spectra from 20 contiguous pixels; this is not possible using macrotechniques. Thermal processing on an ATR crystal is not possible, but casting a film on polished stainless steel using a small-diameter needle allows spectroscopic examination of the entire film before and after heating. Point probing with ATR is less reliable because of its dependence on specific target selection. Imaging allows characterization of the entire area and selection of multiple spectra from pixels selected within the film.

LITERATURE CITED

(1) Ambrose, E. J.; Elliott, A. Infra-red spectroscopic studies of globular protein structure. *Proc. R. Soc.* **1951**, *208A*, 75–90.

(2) Clark, A. H.; Sauderson, D. H. P.; Suggett, A. Infrared and laser-Raman spectroscopic studies of thermally induced globular protein gels. *Int. J. Pept. Protein Res.* **1981**, *17*, 353–364.

(3) Boye, J. I.; Alli, I.; Ismail, A. A.; Gibbs, B. F.; Konishi, Y. Factors affecting molecular characteristics of whey protein gelation. *Int. Dairy J.* **1994**, *5*, 337–353.

(4) Payne, K. J.; Veis, A. Fourier transform IR spectroscopy of collagen and gelatin solutions: deconvolution of the amide I band for conformational studies. *Biopolymers* **1988**, *27*, 1749–1760.

(5) Haris, P. I.; Severcan, F. FTIR spectroscopic characterization of protein structure in aqueous and non-aqueous media. *J. Mol. Catal. B: Enzymatic* **1999**, *7*, 201–221.

(6) Lefévre, T.; Subirade, M. Structural and interaction properties of β-lactoglobulin as studied by FTIR spectroscopy. *Int. J. Food Sci. Technol.* **1999**, *34*, 419–428.

(7) Byler, D. M.; Purcell, J. M. FTIR examination of thermal denaturation and gel formation in whey proteins. *SPIE, Fourier Transform Spectrosc.* **1989**, *1145*, 415–417.

(8) Choo, L. P.; Wetzel, D. L.; Halliday, W. C.; Jackson, M.; LeVine, S. M.; Mantsch, H. H. *In situ* characterization of β-amyloid in Alzheimer's diseased tissue by synchrotron Fourier transform infrared microspectroscopy. *Biophys. J.* **1996**, *71*, 1672–1679.

(9) Wetzel, D. L.; Srivarin, R.; Finney, J. R. Revealing protein infrared spectral detail in a heterogeneous matrix dominated by starch. *Vib. Spectros.* **2003**, *31*, 109–114.

(10) Bonwell, E. S.; Fisher, T.; Fritz, A.; Wetzel, D. L. Determination of endosperm protein secondary structure in hard wheat breeding lines using synchrotron infrared microspectroscopy. *Vib. Spectrosc.* **2008**, *48*, 76–81.

(11) Bonwell, E. S. Determination of endosperm protein secondary structure in hard wheat breeding lines using synchrotron infrared microspectroscopy and revelation of secondary structural changes in protein films with thermal processing. MS Thesis, Kansas State University, **2008**.

absorptions occurred at 1650–1670 cm^{-1}; one of the seven occurred at 1620 cm^{-1}. Three films were cast of the water-soluble portion from a single sample of vital wheat gluten. In this case, the initially probed amide I position was prevalently at 1647 cm^{-1}. Upon heating, two of the four amide I bands appeared at 1667 cm^{-1}, and the third appeared at 1655 cm^{-1}.

Use of highly polished stainless steel as an optically reflective substrate to study changes in protein secondary structure during thermal processing is warranted. Its infrared reflectivity lags behind an aluminum mirror, but it is unchanged during heating. This simple, relatively rapid method permits the recording of spectra at the same location of protein films before and after heating. Prior to heating, distribution of the amide I peak maxima
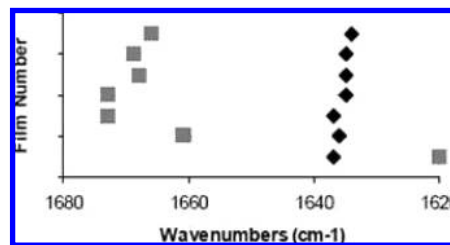
10072 *J. Agric. Food Chem.,* Vol. 57, No. 21, 2009

Bonwell and Wetzel

(12) Meeserman, F.; Smeller, L.; Heremans, K. Comparative Fourier transform infrared spectroscopy study of cold-, pressure-, and heat-induced unfolding and aggregation of myoglobin. *Biophys. J.* **2002**, *82*, 2635–2644.

(13) Georget, D. M. R.; Belton, P. S. Effects of temperature and water content on the secondary structure of wheat gluten studied by FTIR spectroscopy. *Biomacromolecules* **2006**, *7*, 469–475.

(14) Bruun, S. W.; Sondergaard, I.; Jacobsen, S. Analysis of protein structures and interactions in complex food by near-infrared spectroscopy. 2. Hydrated gluten. *J. Agric. Food Chem.* **2007**, *55*, 7244–7251.

(15) Elmore, D. L.; Smith, S. A.; Lendon, C. A.; Muroski, A. R. Probing the structural effects of pasteurization and spray drying on soy protein isolate in the presence of trehealose using FT-IR-ATR and FT-Raman spectroscopy. *Spectroscopy* **2007**, *22*, 38–44.

(16) Prudêncio-Ferreira, A. H.; Arêas, J. A. G. Protein−protein interactions in the extrusion of soya at various temperatures and moisture contents. *J. Food Sci.* **1993**, *58*, 378–384.

(17) Jackson, M.; Mantsch, H. H. The use and misuse of FTIR spectroscopy in the determination of protein structure. *Crit. Rev. Biochem. Mol. Biol.* **1995**, *30*, 95–120.

(18) Jackson, M.; Mantsch, H. Artifacts associated with the determination of protein secondary structure by ATR-IR spectroscopy. *Appl. Spectrosc.* **1992**, *46*, 699–701.

(19) Nabet, A.; Pézolet, M. Two-dimensional FT-IR spectroscopy: a powerful method to study the sencenary structure of proteins using H−D exchange. *Appl. Spectrosc.* **1997**, *51*, 466–469.

(20) Yang, W. J.; Griffiths, P. R.; Byler, D. M.; Susi, H. Protein conformation by infrared spectroscopy resolution enhancement by Fourier self-deconvolution. *Appl. Spectrosc.* **1985**, *39*, 282–287.

(21) Byler, D. M.; Susi, H. Examination of the secondary structure of proteins by deconvolved FTIR spectra. *Biopolymers* **1986**, *25*, 469–487.

(22) Haris, P. I.; Chapman, D. Does Fourier-transform infrared spectroscopy provide useful information on protein structures? *Trends Biochem. Sci.* **1992**, *17*, 328–333.

(23) Smeller, L.; Rubens, P.; Heremans, K. Pressure effect on temperature-induced unfurling and tendency to aggregate of myoglobin. *Biochemistry* **1999**, *38*, 3816–3820.

(24) Evans, S. V.; Brayer, G. D. High-resolution study of the three dimensional structure of horse heart metmyoglobin. *J. Mol. Biol.* **1990**, *213*, 885–897.